International Society for Rock Mechanics and Rock Engineering
Norwegian Group for Rock Mechanics

ISRM International Symposium
Eurock 2025 – Expanding the Underground Space
Trondheim, Norway, 16-20 June
ISBN 978-82-8208-079-8

Dynamic Tensile Response of Rock-Lining Interface with Varying JRC Profiles

A. Mohapatra[1], S. Kashyap[1], S. Mishra[1] & W. Chen[2]
[1]*Department of Mining Engineering, Indian Institute of Technology, Kharagpur, India*
[2]*School of Civil and Mechanical Engineering, Curtin University, Australia.*
smishra@mining.iitkgp.ac.in

Abstract

Concrete, whether used as segmental lining or shotcrete around an underground opening in rock mass, is crucial for the overall stability of structures such as tunnels, underground mines, roadways, energy storage reservoirs, and underground chambers (Guo et al., 2023). These structures are often subjected to unexpected dynamic loads which may arise from natural hazards like earthquakes, or man-made hazards such as bomb blasts, missile attacks, or collisions (Mishra et al., 2016). These extreme loading events, whether natural or man-made, propagate as stress waves through the rock-lining interface and induces high rates of loading leading to catastrophic failures. It is known that the rock is weak under tensile, and the rock-lining interface is particularly sensitive to tensile loading resulting in dynamic tensile failure in the tangential direction at the interface. The tensile behavior of the rock-lining interface has been extensively studied in the literature with typical sawtooth angles both under low and high loading conditions. However, the dynamic tensile response of a rock-lining interface with varying JRC profiles (Barton & Choubey, 1977) has seldom been studied in literature. The present study focuses on performing numerical simulations on the rock-lining interface with varying JRC profiles. Three-dimensional finite element numerical models of the rock concrete interface with different JRC profiles will be developed similar to the experimental test set-up for dynamic tensile loading as given in Zhu et al. (2020) using the commercially available finite element software, ABAQUS. The dynamic tensile behaviour of the interface will be investigated along with the effect of interface roughness and the failure modes under varying strain rate loading conditions. This data would be helpful in the safe designing of underground structures under multi-hazard loading conditions.

Keywords

Dynamic Tension, JRC, Numerical Model, Rock-lining Interface, SHPB

1 Introduction

The construction of tunnels has been a focal point worldwide for some time, with the choice of tunnel lining material being a critical factor that governs the stability of underground infrastructure. Among various lining materials, shotcrete plays a significant role in stabilizing the surrounding rock of underground excavations by creating an interface between the rock and concrete. This interface is highly sensitive to loading conditions, often leading to structural failures originating at this point. The rock-lining interface is particularly vulnerable to tensile loading, which is a primary cause of structural instability, resulting in inclined cracks, concrete spalling, or even the complete collapse of underground openings (Roy and Sarkar, 2017). In addition to static loads, such as crustal stress or overburden pressure, the rock-lining interface is also subjected to dynamic loads, including seismic events, blasting operations, or vibrations from machinery operations (Zhu et al., 2020). While the static response of the rock-lining interface has been extensively studied, there is limited understanding of its dynamic tensile properties, particularly regarding failure mechanisms and failure modes.

Numerous researchers have made significant contributions to understanding the mechanical behavior of rock-concrete structures under static tensile loading conditions. For instance, Kuchta (2002) studied the impact of surface roughness on the interface strength of shotcrete and found that surface treatment enhances interface strength. Ozturk and Tannant (2010, 2011) examined the effects of substrate parameters, such as tensile strength, surface roughness, grain size, and contaminants like oil and dust, on the interface strength between shotcrete and rock mass. Their findings showed that, under static indirect tension, contaminants degrade interface strength, while larger grain sizes increase the adhesive strength of the rock-concrete interface. Son (2013) conducted various tests—direct tension, split tension, and flexural tension—to assess the adhesive strength of the rock-concrete interface under static tensile loading. Well, these studies were primarily limited to quasi-static conditions. Chang et al. (2018) performed static Brazilian Disc (BD) tests to investigate how loading directions affect the adhesive properties of the rock-concrete interface. They identified three distinct failure patterns in composite specimens based on loading orientation. Their results demonstrated that as the interface angle increases, the failure mode transitions progressively from shear failure to a combined tensile-shear failure, and ultimately to tensile failure.

In addition to static tensile loads, rock-concrete structures are often subjected to dynamic loads, such as earthquakes and blasting events (Deng et al., 2014). However, limited research has been conducted on the cohesive behavior of the rock-concrete interface under dynamic tensile conditions. The only notable study in this area was by Luo et al. (2017), who investigated the mechanical properties of bi-material discs under dynamic loading. Their study focused solely on interface roughness, characterized by sawtooth widths of 1.25 mm and depths of 0 mm, 0.6 mm, 1.2 mm, 1.8 mm, 2.4 mm, and 3.0 mm, and its effect on tensile strength. The findings showed that tensile strength initially increased and then decreased with increasing interface roughness. The orientation of the interface in their experiments was parallel to the loading direction. However, in practical engineering applications, the orientation of the rock-concrete interface often deviates from the load direction. Furthermore, the study used a simplified sawtooth interface geometry, which does not fully replicate the natural characteristics of rock-concrete interfaces. More importantly, a systematic investigation of the dynamic response at the rock-concrete interface, incorporating different joint roughness coefficient (JRC) values that better replicate natural interfaces has never been done in the literature. Therefore, it is crucial to study the mechanical response of the rock-concrete interface under dynamic tensile loading with various JRC profiles for both academic and engineering relevance.

In the present study, the rock-concrete interface is simulated numerically using various Joint Roughness Coefficient (JRC) profiles as defined by Barton and Choubey (1977). Three-dimensional finite element models of the rock-concrete interface are developed, incorporating three different JRC profiles of 2-4, 8-10, and 18-20, based on the experimental setup for dynamic tensile loading as described in Zhu et al. (2020). These models are created using the commercially available finite element software ABAQUS. The rock type selected for this study is granite, while C30 grade shotcrete is used as lining material. The strain rate-dependent Drucker-Prager constitutive model is applied to the rock domain, whereas the Concrete Damage Plasticity (CDP) model is used for the concrete domain. The dynamic tensile behavior of the interface is analyzed focusing on the effects of interface roughness under varying strain rate loading conditions.

2 Material and Methods

2.1 Constitutive Model

2.1.1 Drucker-Prager Model

The strain rate-dependent Drucker Prager constitutive relation is effectively being used to capture the behaviour of the rock domain i.e. granite. The model considers all the three stress invariants and allows the yield surface to grow in the deviatoric plane with non-circular properties. The yield criterion for the Drucker-Prager model is shown in Equations 1 and 2:

$$F = t - p\tan\beta - d = 0 \tag{1}$$

where,

$$t = \frac{1}{2}q\left[1 + \frac{1}{K} - \left(1 - \frac{1}{K}\right)\left(\frac{r}{q}\right)^3\right] \tag{2}$$

where, β is the slope of the linear yield surface in the *p*-*t* stress plane, *d* is the cohesion of the material, *p* is the equivalent pressure stress, *q* is the von Mises equivalent stress, *r* is the third invariant of deviatoric stress, *K* is the ratio of the yield stress in triaxial tension to the yield stress in triaxial compression. When $K = 1$, $t = q$, indicating that the yield surface forms the von Mises circle in the deviatoric principal stress plane (the π-plane). To maintain convexity of the yield surface, it is necessary to ensure that $0.778 \leq K \leq 1.0$.

2.1.2 Concrete Damage Plasticity Model

The strain rate-dependent Concrete Damaged Plasticity (CDP) model is used to simulate the behavior of the concrete domain, which serves as the lining material in this study. This model effectively captures the compressive crushing and tensile cracking of brittle materials like concrete. A key feature of the CDP model is its use of a smeared crack approach, where individual micro-cracks are not tracked explicitly. Instead, the model performs constitutive calculations independently at each integration point of the finite element model.

In the CDP model, the compressive stress-strain relationship is linear up to the yield stress, after which it enters the plastic regime, exhibiting strain hardening until the ultimate stress is reached. In contrast, the tensile stress-strain behavior remains linear up to the ultimate stress, beyond which it enters a softening regime (Chaudhary et al., 2019). The stress-strain relationships for the Concrete Damage Plasticity model (equations (3) and (4)) are as follows:

$$\sigma_c = \frac{(1-d_c)D_0^{el}}{(\varepsilon - \varepsilon_c^{pl})} \tag{3}$$

$$\sigma_t = \frac{(1-d_t)D_0^{el}}{(\varepsilon - \varepsilon_t^{pl})} \tag{4}$$

where *c* and *t* refer to the compression and tension behaviour, respectively, d_c represents compression damage variable, d_t represents tension damage variable, and D_0^{el} represents initial (undamaged) elasticity matrix. The σ_c represents compressive stress and σ_t represents tensile stress; ε_c^{pl} and ε_t^{pl} are compressive and tensile plastic strains, respectively.

2.2 Validation of Constitutive Models

The numerical model is validated with the experimental results taken from Zhu et al. (2020). In the experimental study, Zhu et al. (2020) observed the mechanical response of the rock-shotcrete interface under dynamic tensile loading conditions using the split Hopkinson pressure bar (SHPB) device for different sawtooth angles made in Brazilian disc (BD) specimens. Hence, as shown in Fig. 1 (a), a three-dimensional finite element (FE) model similar to the experimental set-up along with the rock-shotcrete BD specimen is developed using ABAQUS. The BD specimen is modeled with the upper

half as granite, the lower half as C30 shotcrete, and the interface with different sawtooth angles (i.e., 0° (flat interface), 15°, 30° and 45°). The detailed view of the FE model of the BD specimen is also shown in Fig. 1 (b). The strain rate-dependent Drucker-Prager constitutive model is used to capture the stress-strain behavior of granite rock, whereas the Concrete Damage Plasticity (CDP) model is used to capture the stress-strain behavior of C30 grade shotcrete. The input parameters for the Drucker-Prager constitutive model used in the present study are presented in Table 1 and the input parameters for the Concrete Damage Plasticity model used in the present study are presented in Table 2, where f_{b0}/f_{c0} is the ratio initial equibiaxial compressive stress to initial uniaxial compressive stress and K is the ratio of second stress invariant on the tension meridian to that on the compressive meridian at initial yield.

Table 1 Constitutive model parameters used for Drucker-Prager (DP) model.

Constitutive Model	**Shear Criterion**	**Eccentricity (e)**	**Friction Angle (β), degree**	**Flow stress ratio (K)**	**Dilation Angle (ψ), degree**
Drucker-Prager	Linear	0.1	42.5	0.778	5.3

Table 2 Constitutive model parameters used for the Concrete Damage Plasticity (CDP) model.

Constitutive Model	**Dilation Angle (ψ), degree**	**Flow potential Eccentricity (e)**	f_{b0}/f_{c0}	K	**Viscosity Parameter (μ)**
Concrete Damage Plasticity	35	0.1	1.16	0.667	0

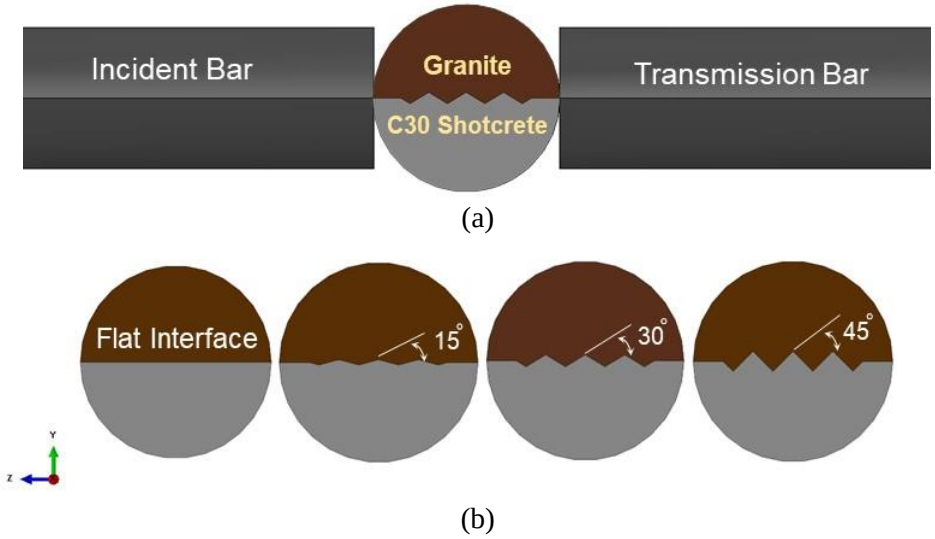

Fig. 1 (a) Schematic diagram of the numerical model similar to the experimental set-up of Zhu et al. (2020), (b) Models of rock-shotcrete specimens with different sawtooth dip angles.

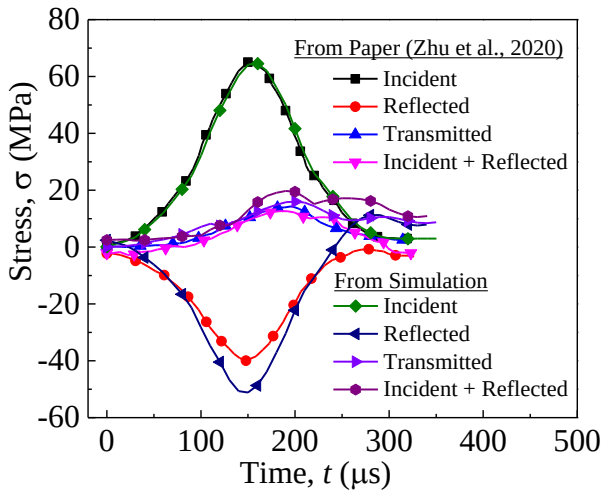

Fig. 2 Validation plot for dynamic stress equilibrium obtained from numerical simulation with experimental test results of 15° sawtooth angle interface.

Figure 2 shows the numerical validation of the stress equilibrium results observed during the dynamic tensile test on a rock-concrete specimen with a 15° sawtooth angle interface (Zhu et al., 2020). The numerical results indicate that, prior to reaching the peak of the transmitted stress, the sum of the incident and reflected stresses is approximately equal to the transmitted stress, consistent with the experimental findings of Zhu et al. (2020). This suggests that the rock-concrete specimen was in a state of dynamic stress equilibrium before failure occurred.

2.3 Modelling of rock-shotcrete interface with different JRC profiles

After the numerical validation study of different sawtooth angles, a similar 3D finite element model is developed using ABAQUS. Instead of varying sawtooth angles at the interface between the rock and shotcrete, JRC profiles defined by Barton and Choubey (1977) (i.e., JRC 2-4, 8-10, and 18-20) are applied as the interface between the rock and shotcrete specimen. The validated strain rate-dependent Drucker-Prager constitutive model is used to model the rock, while the Concrete Damage Plasticity (CDP) model is used for the shotcrete to capture their respective stress-strain behaviours. The same granite and C30-grade shotcrete are used for the rock-shotcrete specimen. The modelled rock-shotcrete Brazilian Disc (BD) specimen has a diameter of 50 mm and a thickness of 25 mm. The incident and transmitted bars are modelled with lengths of 3000 mm and 1800 mm, respectively, both having a diameter of 38.1 mm. The boundary conditions for modelling SHPB tests with one-dimensional stress wave propagation and fixed transmission bar end is applied to the developed model. The far end of the transmitted bar is fixed in all three directions and in all axes of rotation, i.e., $U_x = U_y = U_z = 0$. Figure 3 shows the numerical model of the dynamic tensile test with the Split Hopkinson Pressure Bar (SHPB) setup for testing a rock-shotcrete specimen with the JRC profile as the interface. A detailed view of the meshed finite element model of the rock-shotcrete specimen with the JRC profile interface is shown in Figure 4. The 3D mesh of the SHPB test setup is developed by using an eight-node brick element (C3D8R) with reduced integration, hourglass control, and finite membrane strains. For maintaining the accuracy of analysis, mesh convergence studies are performed with the incorporation of higher mesh density towards the center of the test setup. A mesh sensitivity analysis was also performed, and it was seen that the results started to converge with finer mesh of 0.2 mm element size and least computation time. The general contact option in Abaqus is used to model the contact between the bar and the specimen with hard contact in the normal direction and frictionless contact in the tangential direction. The input properties for the FE model of the rock-shotcrete specimen are provided in Table 3.

Table 3 Input properties for FE model of the rock-shotcrete BD specimen.

Rock	**Density (ρ), kg/m^3**	**Young's Modulus (E), GPa**	**Poisson's Ratio (ν)**
Granite	2634.38	47.11	0.23
C30 Shotcrete	2450	29.45	0.20

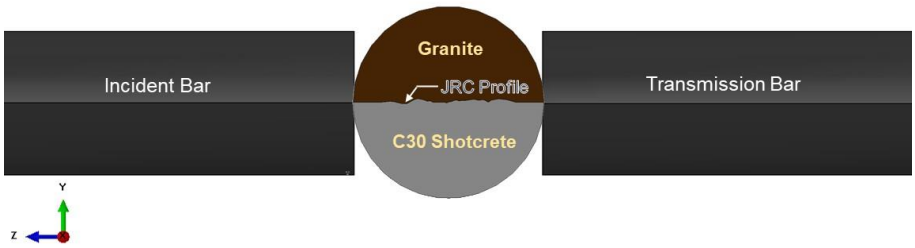

Fig. 3 Numerical model of the dynamic tensile test with SHPB setup to test a rock-shotcrete specimen with the JRC profile as the interface.

The numerical simulations are performed at a loading rate of 400 GPa/s as derived from the incident pulse shown in Figure 2. This loading rate is obtained using a striker bar length of 100 mm length and 38.1 diameter.

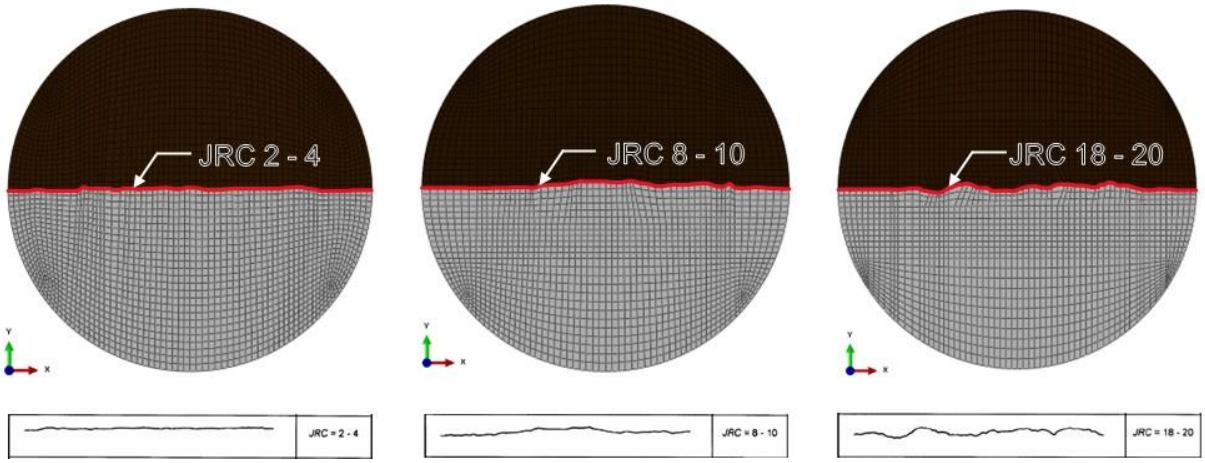

(a) (b) (c)

Fig. 4 Meshed FEM model of rock-shotcrete specimen with different JRC profiles as given by Barton and Choubey (1977) (a) JRC 2-4 (b) JRC 8-10 (c) JRC 18-20.

3 Results and Discussion

The stress wave pulses recorded from the central element on the incident and transmitted bars surfaces and the post-processed dynamic stress equilibrium obtained from those recorded stress pulses for a typical rock-shotcrete 2-4 JRC profile interface are shown in Fig. 5 (a) and (b). It can be clearly seen from Figure 5 (b) that the stress equilibrium is achieved in the numerical simulation considering the analysis to be valid.

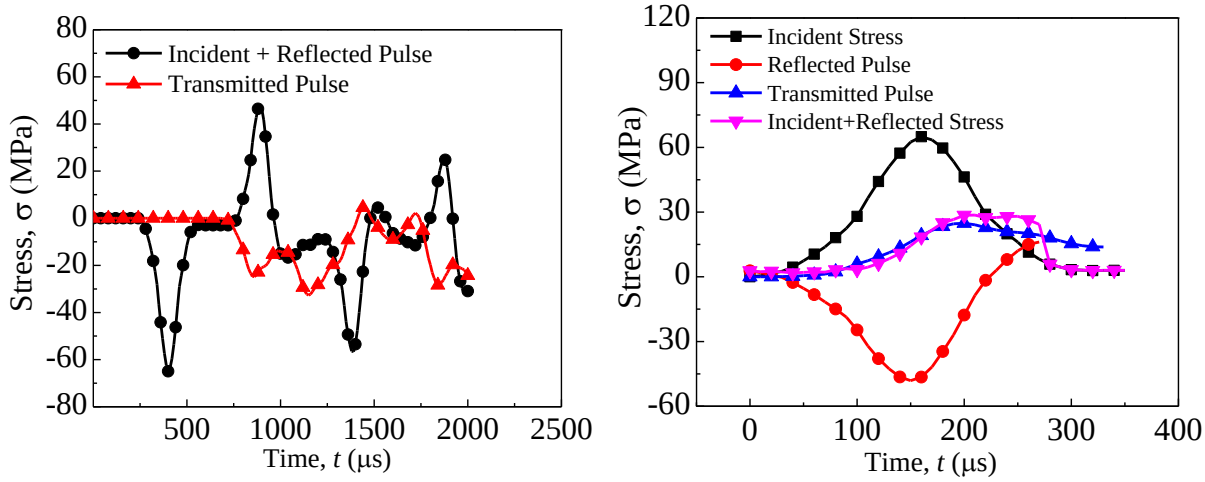

(a) (b)

Fig. 5 (a) Stress pulses and (b) dynamic stress equilibrium plot for a rock-shotcrete 2-4 JRC profile interface.

The stress-time graphs and stress-strain responses of rock-shotcrete BD specimens with different joint roughness coefficients (JRC) obtained from numerical analysis performed under dynamic loading conditions are shown in Figures 6(a) and 6(b), respectively. It can be clearly seen from Figure 6(a) and 6(b) that the peak tensile strength obtained by JRC 18–20 BD specimen, i.e., 14.81 MPa is slightly higher than that of JRC 2–4 and 8–10 BD specimens. However, the peak strength obtained by JRC 2-4 and JRC 8-10 BD specimen is almost similar. Hence, it is well understood that the tensile stress response improves with higher values of JRC due to its better mechanical interlocking and roughness at the rock-shotcrete interface, thereby providing resistance to the loading rate resulting in slightly enhanced stress values. In contrast, smoother interfaces (lower JRC) exhibit delayed stress buildup and lower peak stress values due to limited interfacial interlocking, underlining the critical role of surface roughness in dynamic tensile performance.

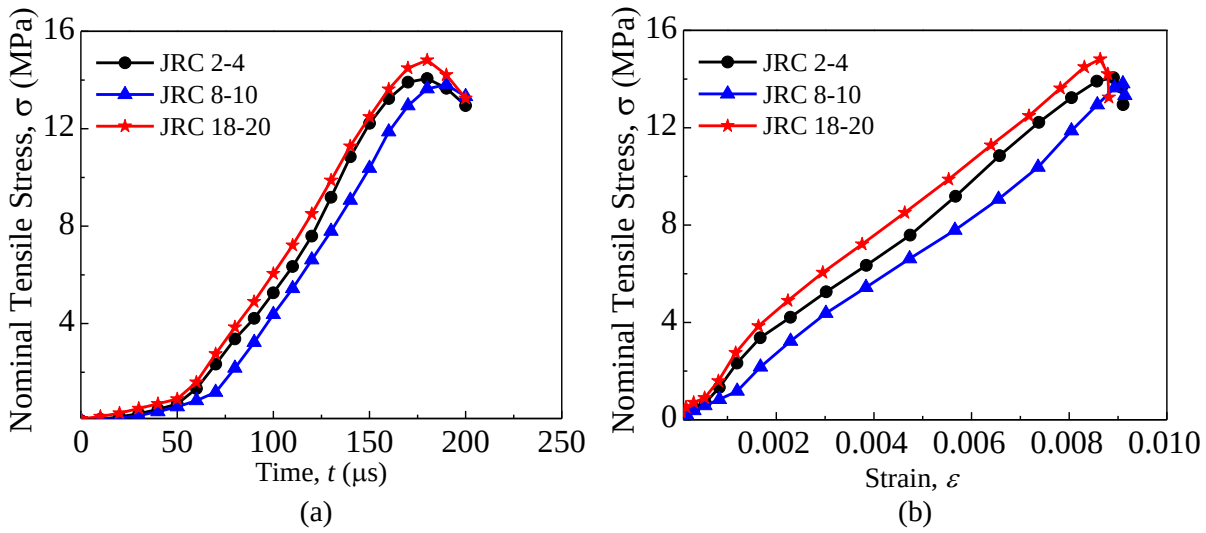

Fig. 6 (a) Nominal tensile stress vs time plot (b) Nominal tensile stress vs strain plot for different JRC values at the interface between rock-shotcrete specimen

4 Conclusion

It is concluded that there exists an influence of interface roughness on the dynamic tensile behaviour of rock-lining interface. The present study numerically assessed the resistance of rock-lining interface to dynamic tensile loading by employing Joint Roughness Coefficient (JRC) profiles of 2–4, 8–10, and 18–20 at the rock-shotcrete interface as proposed by Barton and Choubey (1977). The numerical results showed that the higher the JRC value, the more significant is the nominal tensile strength in dynamic loading conditions. In particular, JRC 18–20 has superior mechanical behavior with a higher peak stress at a shorter time as compared to JRC 2–4 and JRC 8–10. This is due to improved mechanical interlocking at rougher interfaces, which enables efficient stress transfer and energy dissipation. For smoother interfaces (lower JRC values), delayed stress buildup and lower peak stresses are seen because of limited interfacial interlocking. Results indicate that interface roughness plays a critical role in improving the dynamic tensile behavior of rock-shotcrete specimens highlighting its importance for practical applications in multi-hazard scenarios involving dynamic loads.

References

ABAQUS (2023) Dassault Systemes Simulia Corporation, Providence, RI, USA.

Barton N, Choubey V (1977) The shear strength of rock joints in theory and practice. Rock Mechanics 10: 1-54. https://doi.org/10.1007/BF01261801.

Chang X, Lu J, Wang S, Wang S (2018) Mechanical performances of rock-concrete bi-material disks under diametrical compression. International Journal of Rock Mechanics and Mining Sciences 104: 71-77.

Chaudhary RK, Mishra S, Chakraborty T, Matsagar V (2019) Vulnerability analysis of tunnel linings under blast loading. International Journal of Protective Structures 10(1): 73-94. https://doi.org/10.1177/2041419618789438.

Deng XF, Zhu JB, Chen SG, Zhao ZY, Zhou YX, Zhao J (2014) Numerical study on tunnel damage subject to blast-induced shock wave in jointed rock masses. Tunnelling and Underground Space Technology 43: 88-100.

Kuchta, ME (2002). Quantifying the increase in adhesion strength of shotcrete applied to surfaces treated with high-pressure water. Transactions-Society for Mining Metallurgy and Exploration Incorporated 312: 129-132.

Luo L, Li X, Tao M, Dong L (2017) Mechanical behavior of rock-shotcrete interface under static and dynamic tensile loads. Tunnelling and Underground Space Technology 65: 215-224.

Ozturk H, Tannant DD (2010) Thin spray-on liner adhesive strength test method and effect of liner thickness on adhesion. International Journal of Rock Mechanics and Mining Sciences 47 (5): 808–815.

Ozturk H, Tannant DD (2011) Influence of rock properties and environmental conditions on thin spray-on liner adhesive bond. International Journal of Rock Mechanics and Mining Sciences 48 (7): 1196–1198.

Roy N, Sarkar R (2017) A review of seismic damage of mountain tunnels and probable failure mechanisms. Geotechnical and Geological Engineering 35: 1-28.

Son M (2013) Adhesion strength at the shotcrete–rock contact in rock tunneling. Rock Mechanics and Rock Engineering 46: 1237-1246. DOI 10.1007/s00603-013-0380-0.

Zhu J, Bao W, Peng Q, Deng X (2020) Influence of substrate properties and interfacial roughness on static and dynamic tensile behaviour of rock-shotcrete interface from macro and micro views. International Journal of Rock Mechanics and Mining Sciences 132: 104350. DOI: 10.1016/j.ijrmms.2020.104350.